Surface & Coatings Technology 228 (2013) S323–S327

Contents lists available at SciVerse ScienceDirect

Surface & Coatings Technology

journal homepage: www.elsevier.com/locate/surfcoat

Improved field electron emission from SiC assisted carbon nanorod/nanotube heterostructured arrays by using energetic Si ion irradiation

Jian-hua Deng [1], Peng-cheng Sun [1], Guo-an Cheng *[,1], Rui-ting Zheng [1]

Key Laboratory of Beam Technology and Material Modification of the Ministry of Education, College of Nuclear Science and Technology, Beijing Normal University, Beijing 100875, P. R. China

ARTICLE INFO

Available online 2 June 2012

Keywords:
Multiwall carbon nanotube arrays
Silicon ion irradiation
Field emission
Stability behavior

ABSTRACT

Field electron emission characteristics of energetic silicon ion irradiated carbon nanotube arrays were investigated. SEM, TEM, Raman, XPS and photoelectron spectrometry characterizations were done for comparison before and after the silicon ion irradiation. Carbon nanorod/nanotube heterostructure is obtained and SiC compound is formed in the carbon nanotubes after the silicon ion irradiation. Silicon ion irradiated carbon nanotube arrays with an irradiation dose of 8.6×10^{16} ions/cm^2 show excellent field emission properties, with low turn-on and threshold fields of 0.726 and 1.164 V/μm, respectively, which are far better than that of the original and the silicon ion irradiated carbon nanotube arrays with other irradiation doses. We attribute the main reason for this field emission enhancement to the change of microstructures of carbon nanotubes, which directly influences the number of emission sites during field emission and additionally, the formation of low work function SiC compound. However, with further increasing the irradiation dose, the field emission characteristics of the carbon nanotube arrays deteriorate for the decrease of emission sites induced by severe structural damage. Furthermore, the silicon ion irradiated carbon nanotube arrays with an irradiation dose of 8.6×10^{16} ions/cm^2 present far better stability than the original carbon nanotubes, providing a possibility for the application of high-performance field emission devices.

1. Introduction

Since their discovery [1], carbon nanotubes (CNTs) have aroused much speculation as field electron emitters due to their high aspect ratio, eminent chemical inertness and superior electrical conductivity [2]. Works on improving field electron emission characteristics of CNTs have been developed widely during the last few years both experimentally and theoretically [3,4], and one of the research focuses is improving the field emission (FE) properties of CNTs by using energetic ion irradiation due to the incomparable controllability of irradiation doses. A report from Lee et al. revealed that the FE characteristics of CNTs were enhanced greatly by exposing them to plasma, and they ascribed this enhancement to the plasma-induced increase of effective emission area of the CNTs [5], and the plasma treatment has also been adopted by some other groups [6,7]. Another study carried out by Kyung et al. found that an evident drop of turn-on electric field (E_{on}, applied field at 10 μA/cm^2) from 1.7 to 0.9 V/μm was obtained when the CNTs were exposed to Ar neutral beam due to less field screening [8,9]. As well known, longtime stable electron emission is indispensable in fabricating CNTs-based field devices, and it has aroused much speculation on this aspect [10,11]. A study from Chen et al. showed a negligible emission current density drop of CNTs at 1 mA/cm^2 in 19 h after a tip sonication pretreatment was carried out, which can effectively cut CNTs short and regulate the length of CNTs [12]. However, researches on promoting the FE properties by forming heterostructure in CNTs are not so numerous, and the exact relationship between the irradiation doses and the structural change of CNT is still an open question.

In this study, based on works we have done previously [13–15], well aligned CNT arrays (CNTAs) were fabricated and consequently processed by energetic Si ion irradiation. Furthermore, the FE characteristics of the Si ion irradiated CNTAs were measured and the relationship between the irradiation doses and the FE properties was discussed.

2. Experimental section

The thermal chemical vapor deposition (CVD) system used for the synthesis of CNTAs has been previously described in detail [15]. In brief, a 5 nm-thick iron film was deposited first as the catalyst, and ammonia gas, hydrogen and acetylene with a flow ratio of 150:87:600 were used as the etchant, the carbon source and the carrying gas, respectively. The growth of CNTAs was carried out in a tubular furnace at 750 °C in 30 min at the ambient pressure. And then, the prepared

* Corresponding author. Tel./fax: +86 10 62205403.
E-mail addresses: shangdidezhufu@mail.bnu.edu.cn (J. Deng), pcsun@mail.bnu.edu.cn (P. Sun), gacheng@bnu.edu.cn (G. Cheng), rtzheng@bnu.edu.cn (R. Zheng).
[1] Postal address: Xinjiekou Wai Street 19#, College of Nuclear Science and Technology, Beijing Normal University, Beijing 100875, China.

0257-8972/$ – see front matter © 2012 Elsevier B.V. All rights reserved.
doi:10.1016/j.surfcoat.2012.05.109

CNTAs were fixed on a whirling specimen holder and irradiated by Si ions with an average energy of 28 keV at a base pressure of 5×10^{-4} Pa, the incidence angle was 45° and the irradiation doses were 4.3×10^{16}, 8.6×10^{16}, 1.4×10^{17} and 2.1×10^{17} ions/cm^2 respectively.

For the FE measurements, a diode configuration with a moveable anode was employed. The prepared CNTAs were stuck to a copper cylinder by conductive tape as the cathode against a stainless steel plate as the anode, and the distance between them was 2 mm. The FE measurements were carried out in a vacuum chamber with a base pressure of 1×10^{-7} Pa at 288 K (cooled by water). The experimental data was recorded automatically by a computer in terms of emission current versus applied voltage (I–V) with an own designed program. Scanning electron microscope (SEM, Hitachi S-4800), high resolution transmission electron microscope (HRTEM, TECNAI F30), Raman (LavRAM Aramis, wavelength: 633 nm), X-ray photoelectron spectroscopy (XPS, PHI Quantera SXM) and photoelectron spectrometer (AC-2 RIKEM KEIKI) were used to characterize the samples before and after the Si ion irradiation.

3. Results and discussion

Energetic ion irradiation on CNTs introduces structural changes, such as electron/atom collision induced defect generation and atom sputtering [16], excessive energy deposition induced defect annealing [17], nonself element irradiation induced element doping and compound formation [18], phase change [19], and so on. Structural changes of the CNTs are greatly dependent on the irradiation doses.

Fig. 1 shows SEM images of the original and the Si ion irradiated CNTAs at different doses. Fig. 1(a–e) shows the side view images and Fig. 1(f–j) shows the top view images of the CNTs, corresponding with the irradiation doses of (a, f) 0, (b, g) 4.3×10^{16} ions/cm^2, (c, h) 8.6×10^{16} ions/cm^2, (d, i) 1.4×10^{17} ions/cm^2 and (e, j) 2.1×10^{17} ions/cm^2, respectively. Evident structural changes are observed at the top of CNTAs. For convenience, the structural changes of CNTs are described as an evolution from separate to coalescent and then to welding with increasing the irradiation dose. For the original CNTAs, as shown in Fig. 1(a, f), the tips are separate from each other. While for the CNTAs irradiated at low doses shown in Fig. 1(b, c, g, h), coalescence emerges. With further increasing the irradiation dose, welding appears as a signal of excessive energy deposition, as shown in Fig. 1(d, e, i, j). It's worth to mention that there is no such a determinate definition about these three morphologies, for instance, coalescence is just the beginning of welding, but the structural evolution of the Si ion irradiated CNTs from separate to welding with increasing the irradiation dose is undoubted. Furthermore, some extruded CNTs are straightened by the energetic ions, as shown in Fig. 1(b–f), and this straightening effect has been widely studied previously [20,21]. The action range of the incident particles is confined at the top of CNTAs due to the shielding of densely packed CNTs since the incidence angle is 45°.

We employed TEM to observe the fine structures of the Si ion irradiated CNTAs. Fig. 2 shows the TEM images of the Si ion irradiated CNTAs at an irradiation dose of 8.6×10^{16} ions/cm^2. Fig. 2(a, b) shows a low-resolution panoramic view of the CNTs. The tips and the sections near the tips of CNTs have been transformed into nanorods, as clearly seen from the HRTEM image shown in Fig. 2(c), revealing that the nanorod is amorphous. While the amorphization in the upper section of CNTs, about 3–5 μm away from the CNT tips, is not hundred-percent, as shown in Fig. 2(d), the layered structure disappears but the hollow core remains, and the closer to the tips of CNTs, the thinner the hollow core is. However, for the under sections, 6–8 μm away from the CNT bottom end, the CNTs almost remain unchanged. Therefore, a quasi-one-dimensional heterostructured

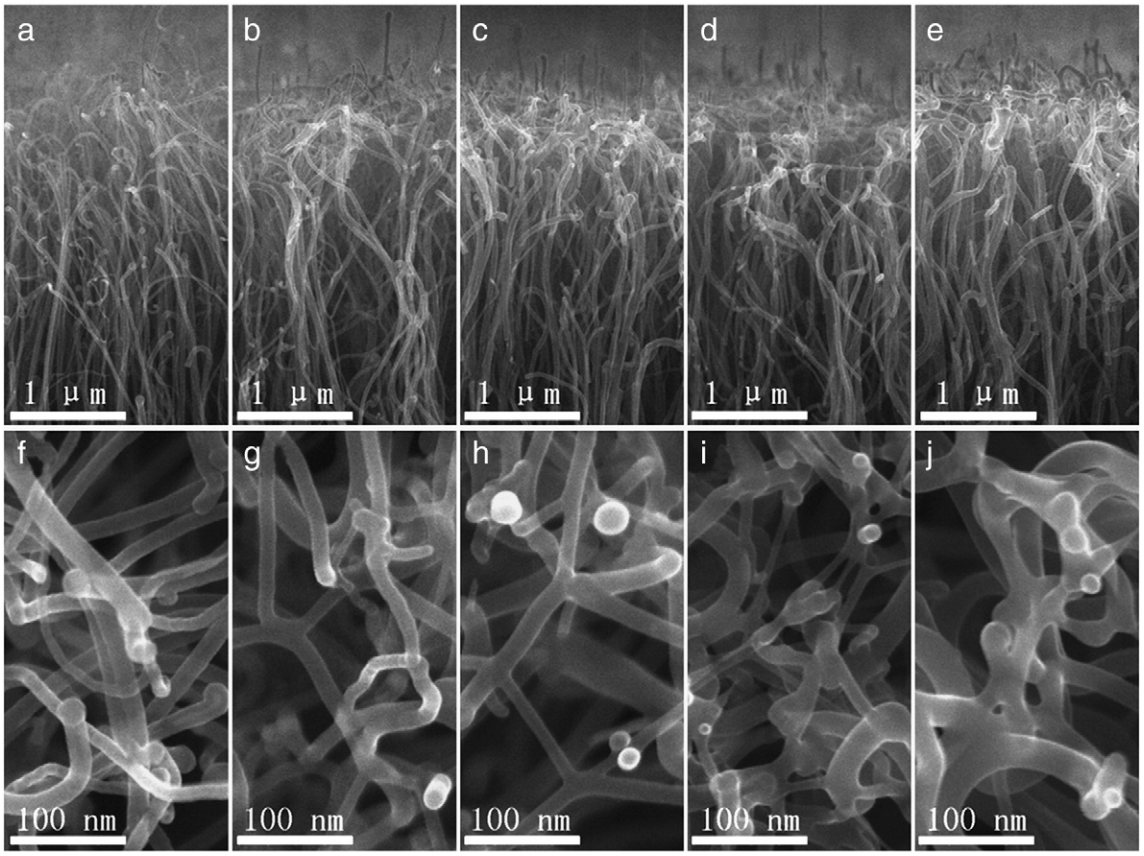

Fig. 1. SEM images of the original and the Si ion irradiated CNTAs at different doses. (a–e) Side view and (f–j) top view images, corresponding with irradiation doses of (a, f) 0, (b, g) 4.3×10^{16} ions/cm^2, (c, h) 8.6×10^{16} ions/cm^2, (d, i) 1.4×10^{17} ions/cm^2 and (e, j) 2.1×10^{17} ions/cm^2, respectively.

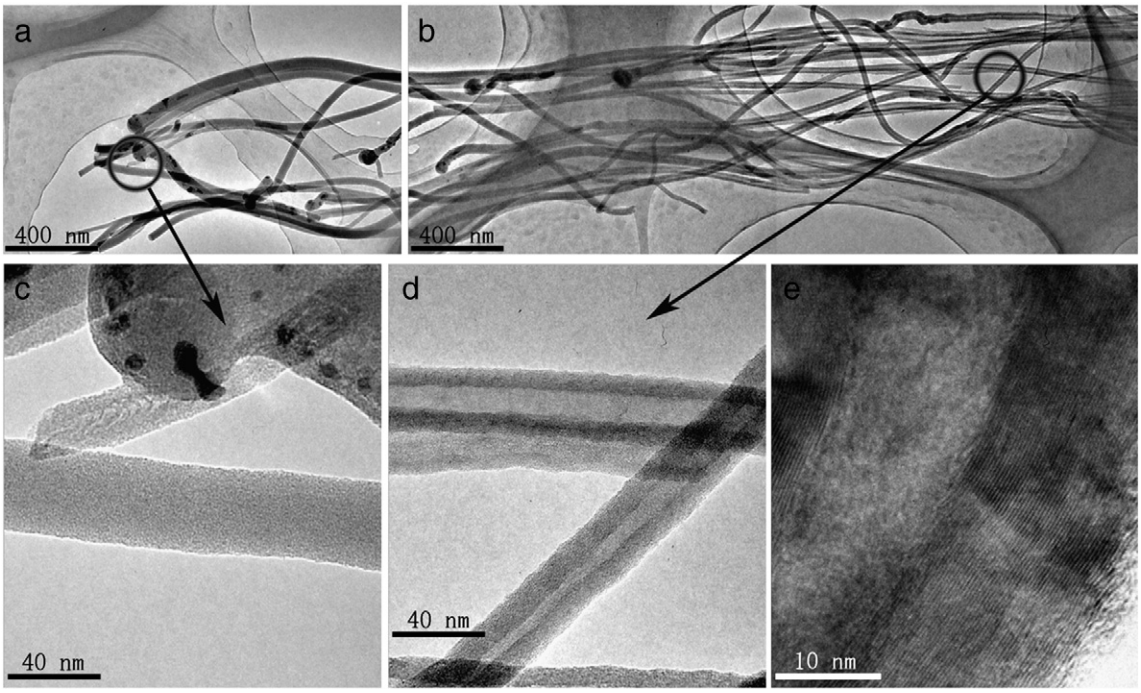

Fig. 2. TEM images of the Si ion irradiated CNTAs with an irradiation dose of 8.6×10^{16} ions/cm^2. (a, b) Panoramic view images. (c) HRTEM image focusing on the tip of CNTs, marked by a circle in image (a). (d) HRTEM image of the upper section of CNTs, marked by a circle in image (b). (e) HRTEM image of the under section of CNTs.

nanorod/nanotube array is obtained by using energetic Si ion irradiation on a CNT array.

The relationship between the structural changes and the irradiation doses was studied by Raman spectroscopy. Fig. 3 shows the Raman spectra of the Si ion irradiated CNTAs with different irradiation doses. The peaks centered at 1335 cm^{-1} and 1586 cm^{-1} are typical defects related D band and crystal graphite related G band, respectively [22]. The intensity ratio of I_D to I_G increases (from 2.77 to 8.15) with increasing the irradiation dose, suggesting that the amorphization of CNTs strongly depends on the irradiation doses and the formation of defective CNTs is at the cost of crystal graphite.

In order to further understand the structural changes in the formation of carbon nanorod/nanotube heterostructure, we employed XPS to determine the chemical structure of the irradiated CNTs. Fig. 4(a) shows the decomposed C1s peaks of the irradiated CNTAs

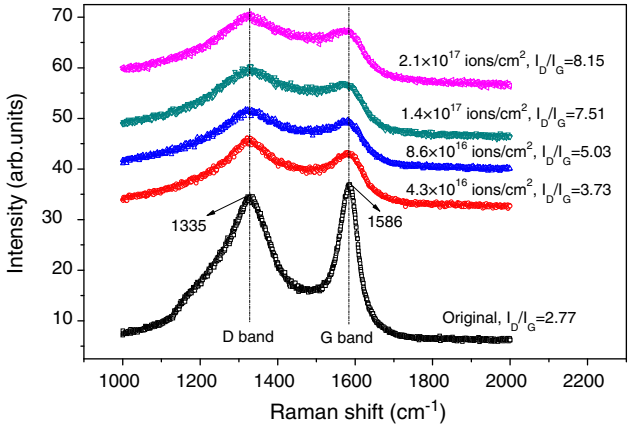

Fig. 3. Raman spectra of the Si ion irradiated CNTAs with different irradiation doses. Wavelength: 633 nm.

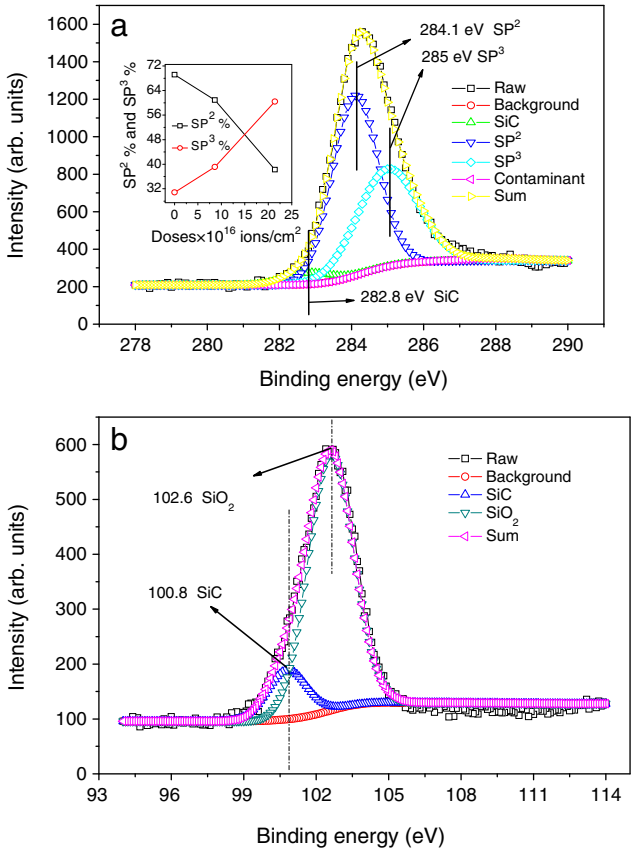

Fig. 4. XPS spectra of the Si ion irradiated CNTAs. (a) Decomposed C1s peaks of the Si ion irradiated CNTAs with an irradiation dose of 8.6×10^{16} ions/cm^2, the inset is the content changes of SP^2- and SP^3-hybridized carbon with increasing the irradiation dose, and (b) decomposed Si2p peaks of the Si ion irradiated CNTAs at an irradiation dose of 8.6×10^{16} ions/cm^2.

with an irradiation dose of 8.6×10^{16} ions/cm^2, peaks centered at 282.8 eV, 284.1 eV, 285 eV and 288 eV are corresponding with SiC compound [23], SP^2-hybridized graphite carbon [24], SP^3-hybridized diamond-like carbon [25] and organic contaminated carbon [26], respectively. The formation of SiC compound can also be evidenced by Fig. 4(b), the decomposed Si2p peak centered at 100.8 eV reveals the existence of SiC compound [27]. The inset of Fig. 4(a) shows the content change of SP^2- and SP^3-hybridized bonds with increasing the irradiation dose. The increase of SP^3-bond (from 30.8% to 60.4%) is found to be at the cost of the decrease of SP^2-bond (from 69.1% to 38.2%), suggesting the amorphization of CNTs, which is in conformity with the Raman analysis. Therefore, the Si ion irradiated CNTAs we obtained can be defined as: SiC compound assisted carbon nanorod/nanotube heterostructured arrays.

Fig. 5(a) shows the FE characteristics of the original and the Si ion irradiated CNTAs with different irradiation doses, given in terms of emission current density versus applied field (J–E). Prior to FE measurements, an aging process was taken when the emission current density was about 10 mA/cm^2 for 5 h to weaken the influence of absorbates induced promotion and Joule-heating induced degradation on the FE characteristics [28–30]. The J–E curves shift to the left (lower applied field) when the irradiation doses are less than 8.6×10^{16} ions/cm^2 and to the right (higher applied field) with further increasing the irradiation dose. This irradiation dose dependent FE of the CNTAs can also be evidenced by the changes of E_{on} and E_{th} (threshold field, applied field at 10 mA/cm^2) shown in Fig. 5(b). The FE properties of the CNTAs are improved (E_{on} from 1.076 to 0.726 V/μm and E_{th} from 1.717 to 1.164 V/μm) by the Si ion irradiation when the irradiation doses are less than 8.6×10^{16} ions/cm^2 but are deteriorated (E_{on} from 0.726 to 1.145 V/μm and E_{th} from 1.164 to 1.828 V/μm) with further increasing the irradiation dose. The inset of Fig. 5(a) is the corresponding FN plots [31], the nearly linear relationship between $\ln(J/E^2)$ and 1/E reveals that the emitted electrons are extracted by the applied fields.

In FN model [31], work function (Φ) and field enhancement factor (β) are two important parameters used for characterizing the FE properties of emitters. In our study, the values of Φ are measured by using photoelectron spectrometer, as shown in Fig. 5(c). The values of Φ are quite different between the original (4.89 eV) and the Si ion irradiated CNTAs (4.67–4.70 eV), and this Φ drop is attributed to the increased state density of defects during ion irradiation induced promotion of the Fermi level [32] and the formation of the low work function material: SiC compound (3.5 eV) [33]. By adopting the FN equation [31], the values of the field enhancement factors (β) are obtained, as shown in Fig. 5(c). The β increases from 4386 to 6139 when the irradiation dose increases from 0 to 8.6×10^{16} ions/cm^2, and then the β decreases from 6139 to 4069 with further increasing the irradiation dose to 2.1×10^{17} ions/cm^2. Comparing the change of β with the variation of FE characteristics of the CNTAs, we find that they both have the same changing trends, and the irradiation dose of 8.6×10^{16} ions/cm^2 is the very watershed, in other words, the ever-changing microstructures of the CNTs are the main reason for the irradiation dose dependent FE properties. β is a parameter strongly dependent on the number of emission sites. When irradiation doses are less than 8.6×10^{16} ions/cm^2, defects, especially vacancy-related defects [34], increase with increasing the irradiation dose,

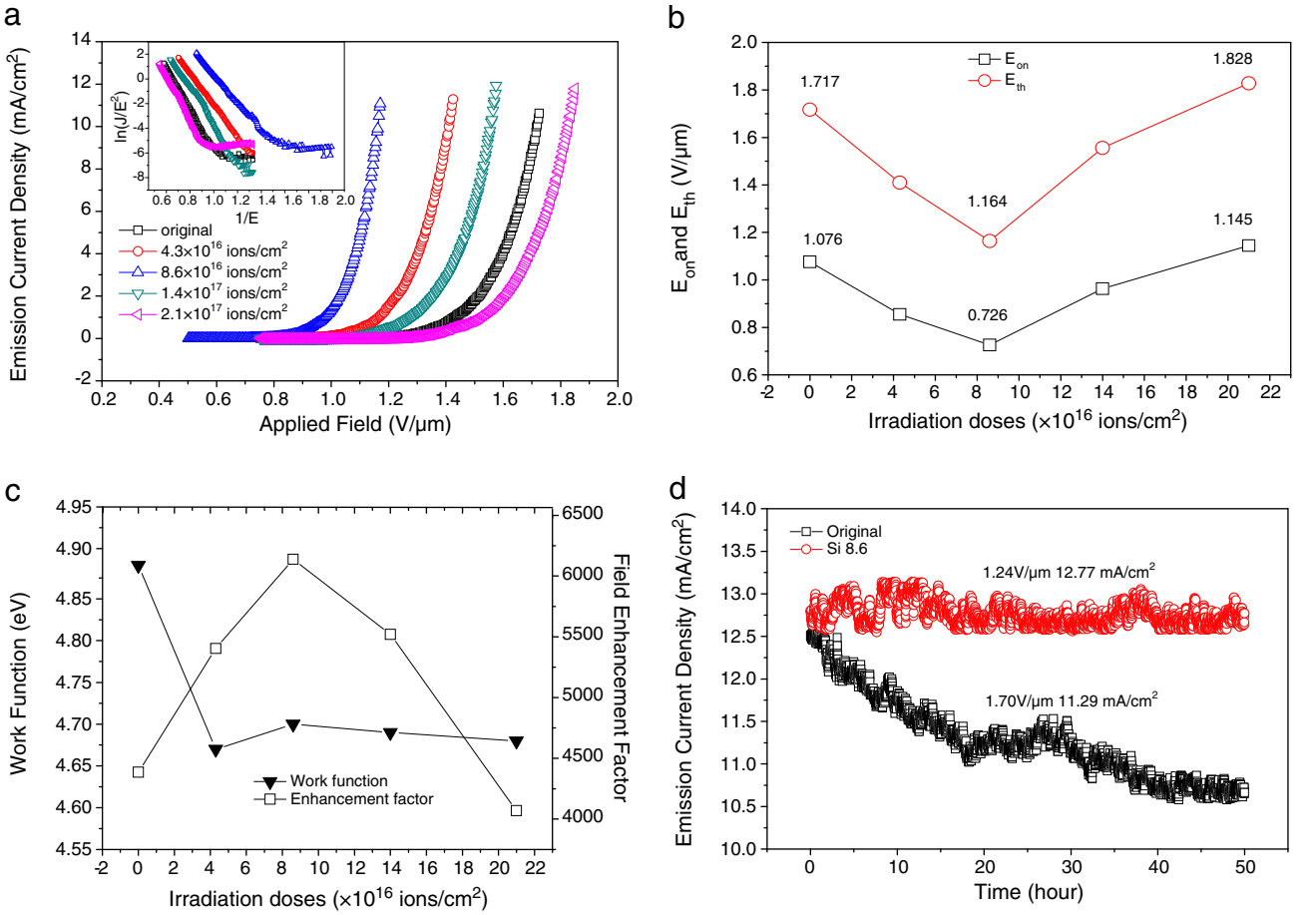

Fig. 5. Field emission characteristics of the original and the Si ion irradiated CNTAs with different irradiation doses. (a) J–E curves and the inset is the corresponding FN plots. (b) The changes of E_{on} and E_{th}. (c) The changes of work function (Φ) and field enhancement factor (β). (d) The stability behavior of the original and the Si ion irradiated CNTAs with an irradiation dose of 8.6×10^{16} ions/cm^2 (Si 8.6).

Table 1
Stability behavior of the original and the Si ion irradiated CNTAs with an irradiation dose of 8.6×10^{16} ions/cm^2 (Si 8.6). E: applied field during, J_{mean}: mean emission current density, J_{drop}: emission current density degradation during stability tests, S_d: standard deviation of the emission current density.

Sample	E (V/μm)	J_{mean} (mA/cm^2)	J_{drop} (%)	S_d/J_{mean} (%)
Original	1.70	11.29	16.32	4.34
Si 8.6	1.24	12.77	0.83	1.04

resulting in the increase of emission sites and thus leading an improvement to the FE characteristics of CNTAs. However, with further increasing the irradiation dose, severe structural damage like welding, as shown in Fig. 1(i, j), may decrease the number of emission sites and deteriorate the FE characteristics of CNTAs. In a word, both the change of microstructures (β) and the change of the Fermi level (Φ) exert influences on the FE properties of the Si ion irradiated CNTAs, but the former is dominative.

Longtime stable field electron emission is essential for the application of FE devices. In this study, 50-hour stability tests of the original and the Si ion irradiated CNTAs with an irradiation dose of 8.6×10^{16} ions/cm^2 (Si 8.6) were carried out, as shown in Fig. 5(d) and Table 1. The mean emission current densities (J_{mean}) of the original and the Si 8.6 CNTAs are 11.29 and 12.77 mA/cm^2, respectively. The applied field (E), the emission current density drop (J_{drop}, $(J_{fisrt}-J_{last})/J_{mean}$, J_{first} and J_{last} are the first and the last mean emission current density during stability tests, respectively), and the ratio of the standard deviation (S_d) and the J_{mean} (S_d/J_{mean}) of the Si 8.6 CNTAs are 1.24 V/μm, 1.83% and 1.04%, respectively, which are much lower than that of the original CNTAs (1.70 V/μm, 16.32%, 4.34%, respectively). The great decrease of applied field (from 1.70 to 1.24 V/μm) is due to the improved FE characteristics of the Si 8.6 sample, as shown in Fig. 5(a). For the other two parameters, J_{drop} and S_d/J_{mean}, which directly reflect the degradation and the fluctuation of the emission current density, the changes are impressive either. As is known to all, ion bombardment introduces structural damages to targets and deposits energy. In this study, great structural changes are observed on the Si ion irradiated CNTAs, as shown in Figs. 1 and 2, some extruded and defective CNTs, which contribute the vast majority of the current degradation during stability tests, are broken off by the incident ions and additionally, the excessive energy deposition induced by ion bombardment anneals part of the unstable defects and stabilizes the emitters, resulting in the decrease of J_{drop}. The fluctuation of emission current density exists during the whole stability tests, as shown in Fig. 5(d). Since a fluctuation is formed by the vanishing of an emission site and the emerging of a new emission site surrounding it, it's thus reasonable to weaken the fluctuation of emission current density by preventing it from degradation. In a word, the bombardment effect on CNTAs induced by Si ion irradiation can effectively strengthen the CNT array and weaken the emission current density degradation and fluctuation, and therefore improve the stability behavior of CNTAs.

4. Conclusions

SiC compound assisted carbon nanorod/nanotube heterostructure has been synthesized by using energetic Si ion irradiation on CVD fabricated CNTAs. Si ion irradiated CNTAs with an irradiation dose of 8.6×10^{16} ions/cm^2 show excellent FE properties, with $E_{on}=0.726$ V/μm, $E_{th}=1.164$ V/μm, which are far better than that of the original CNTAs and CNTAs irradiated with other irradiation doses. We attribute the great improvement of the FE characteristics of Si 8.6 CNTAs to the formation of low work function SiC compound and the structural changes induced by the energetic Si ion irradiation, as evidenced by the increase of the field enhancement factors from 4386 (original) to 6139 (Si 8.6). However, severe damage is brought to CNTAs with further increasing the irradiation dose, which largely decreases the number of emission sites and pose negative influences on the FE characteristics of CNTAs. In addition, 50-hour stability tests of the original and the Si 8.6 CNTAs reveal that energetic ion irradiation is beneficial for realizing stable field electron emission. The J_{drop} of Si 8.6 is only 0.83%, far smaller than that of the original CNTAs (16.32%), suggesting a very promising prospect in the application of CNTAs-based FE devices.

Acknowledgment

This work is supported by the National Basic Research Program of China (no. 2010CB832905), and partially by the Key Scientific and Technological Project of the Ministry of Education of China (no. 108124).

References

[1] S. Iijima, Nature 354 (1991) 56.
[2] R.H. Baughman, A.A. Zakhidov, W.A. de Heer, Science 297 (2002) 787.
[3] L. Xiao, P. Liu, L. Liu, K.L. Jiang, X.F. Feng, Y. Wei, L. Qian, S.S. Fan, T.H. Zhang, Appl. Phys. Lett. 92 (2008) 153108.
[4] S. Shrestha, W.C. Choi, W. Song, Y.T. Kwon, S.P. Shrestha, C.Y. Park, Carbon 48 (2010) 54.
[5] K. Lee, S.C. Lim, Y.C. Choi, Y.H. Lee, Appl. Phys. Lett. 93 (2008) 063101.
[6] Q.H. Wang, T.D. Corrigan, J.Y. Dai, R.P.H. Chang, A.R. Krauss, Appl. Phys. Lett. 70 (24) (1997) 3308.
[7] Y.M. Liu, L. Liu, P. Liu, L.M. Sheng, S.S. Fan, Diamond Relat. Mater. 13 (2004) 1609.
[8] S.J. Kyung, J.B. Park, B.J. Park, J.H. Lee, G.Y. Yeom, Carbon 46 (2008) 1316.
[9] J.S. Suh, K.S. Jeong, J.S. Lee, I. Han, Appl. Phys. Lett. 80 (13) (2002) 2392.
[10] Y.S. Min, E.J. Bae, J.B. Park, U.J. Kim, W. Park, J. Song, C.S. Hwang, N. Park, Appl. Phys. Lett. 90 (2007) 263104.
[11] S.H. Jo, Y. Tu, Z.P. Huang, D.L. Carnahan, J.Y. Huang, D.Z. Wang, Z.F. Ren, Appl. Phys. Lett. 84 (3) (2004) 413.
[12] G.H. Chen, D.H. Shin, S. Kim, S. Roth, C.J. Lee, Nanotechnology 21 (2010) 015704.
[13] F. Zhao, G.A. Cheng, R.T. Zheng, D.D. Zhao, S.L. Wu, J.H. Deng, Nanoscale Res. Lett. 6 (2011) 176.
[14] K.F. Chen, J.H. Deng, F. Zhao, G.A. Cheng, R.T. Zheng, Nanoscale Res. Lett. 5 (2010) 1449.
[15] J.H. Deng, Z.X. Ping, R.T. Zheng, G.A. Cheng, Nucl. Instrum. Methods Phys. Res., Sect. B 269 (2011) 1082.
[16] M.A. Hoefer, P.R. Bandaru, J. Appl. Phys. 108 (2010) 034308.
[17] M. Terrones, H. Terrones, F. Banhart, J.-C. Charlier, P.M. Ajayan, Science 288 (2000) 1226.
[18] C.Y. Zhi, X.D. Bai, E.G. Wang, Appl. Phys. Lett. 81 (9) (2002) 1690.
[19] L.T. Sun, J.L. Gong, D.Z. Zhu, Z.Y. Zhu, S.X. He, Adv. Mater. 16 (20) (2004) 1849.
[20] D.H. Kim, H.S. Jang, C.D. Kim, D.S. Cho, H.D. Kang, H.R. Lee, Chem. Phys. Lett. 378 (2003) 232.
[21] W. Wei, K.L. Jiang, Y. Wei, M. Liu, H.T. Yang, L.N. Zhang, Q.Q. Li, L. Liu, S.S. Fan, Nanotechnology 17 (2006) 1994.
[22] T. Tanabe, Phys. Scr. T64 (1996) 7.
[23] S. Contarini, S.P. Howlett, C. Rizzo, B.A. De Angelis, Appl. Surf. Sci. 51 (1991) 177.
[24] R. Bertoncello, A. Casagrande, M. Casarin, A. Glisenti, E. Lanzoni, L. Mirenghi, E. Tondello, Surf. Interface Anal. 18 (1992) 525.
[25] P. Sundberg, R. Larsson, B. Folkesson, J. Electron. Spectrosc. Relat. Phenom. 46 (1988) 19.
[26] D. Rats, L. Vandenbulcke, R. Herbin, R. Benoit, R. Erre, V. Serin, J. Sevely, Thin Solid Films 270 (1995) 177.
[27] Y. Kanedo, Y. Suginohara, J. Jpn. Inst. Met. 42 (1997) 285.
[28] W.H. Liu, X. Li, C.C. Zhu, Ultramicroscopy 107 (2007) 833.
[29] A. Maiti, J. Andzelm, N. Tanpipat, P. von Allmen, Phys. Rev. Lett. 87 (15) (2001) 155502.
[30] K.A. Dean, T.P. Burgin, B.R. Chalamala, Appl. Phys. Lett. 79 (2001) 1873.
[31] R.H. Fowler, L.W. Nordheim, Proc. R. Soc. London, Ser. A 119 (1928) 173.
[32] G. Kim, B.W. Jeong, J. Ihm, Appl. Phys. Lett. 88 (2006) 193107.
[33] D.A. Da, Vacuum design manual, third ed., National Defence Industry Press, Lanzhou, China, 2004, p. 1620.
[34] G. Wei, Appl. Phys. Lett. 89 (2006) 143111.